ORIGINAL ARTICLE
Cardiovascular Disorders

JKMS

http://dx.doi.org/10.3346/jkms.2013.28.3.402 • J Korean Med Sci 2013; 28: 402-408

Time-Dependent Expression Patterns of Cardiac Aquaporins Following Myocardial Infarction

Hong Zhe Zhang,[1] Moo Hyun Kim,[1] Ju Hyun Lim,[2] and Hae-Rahn Bae[2]

[1]Departments of Cardiology and [2]Physiology, Dong-A University College of Medicine, Busan, Korea

Received: 31 July 2012
Accepted: 4 January 2013

Address for Correspondence:
Hae-Rahn Bae, MD
Department of Physiology, Dong-A University College of Medicine, 36 Dongadae 1-gil, Seo-gu, Busan 602-714, Korea
Tel: +82.51-240-2924, Fax: +82.51-240-2851
E-mail: hrbae@dau.ac.kr

This study was supported by the National Research Foundation of Korea (NRF) grant funded by the Korea Ministry of Education, Science and Technology (MEST) (No. R13-2002-044-04003-0).

Aquaporins (AQPs) are expressed in myocardium and the implication of AQPs in myocardial water balance has been suggested. We investigated the expression patterns of AQP subtypes in normal myocardium and their changes in the process of edema formation and cardiac dysfunction following myocardial infarction (MI). Immunostaining demonstrated abundant expression of AQP1, AQP4, and AQP6 in normal mouse heart; AQP1 in blood vessels and cardiac myocytes, AQP4 exclusively on the intercalated discs between cardiac myocytes and AQP6 inside the myocytes. However, neither AQP7 nor AQP9 proteins were expressed in CD1 mouse myocardium. Echocardiography revealed that cardiac function was reduced at 1 week and recovered at 4 weeks after MI, whereas myocardial water content determined by wet-to-dry weight ratio increased at 1 week and rather reduced below the normal at 4 weeks. The expression of cardiac AQPs was up-regulated in MI-induced groups compared with sham-operated control group, but their time-dependent patterns were different. The time course of AQP4 expression coincided with that of myocardial edema and cardiac dysfunction following MI. However, expression of both AQP1 and AQP6 increased persistently up to 4 weeks. Our findings suggest a different role for cardiac AQPs in the formation and reabsorption of myocardial edema after MI.

Key Words: Myocardial Infarction; Myocytes, Cardiac; Aquaporins; AQP1; AQP4; AQP6

INTRODUCTION

Fluid accumulation in cardiac interstitium has been associated with many diseases or clinical states and results in cardiac dysfunction (1). Myocardial infarction (MI) induces myocardial edema with expansion of both interstitial and intracellular compartments (2). During the ischemia, interstitial edema develops due to the leaky myocardial capillaries, and is followed by swelling and dysfunction of cardiac myocytes (3). The resulting impairment of systolic and diastolic functions is of prognostic importance in the patient survival after myocardial infarction (4, 5).

Aquaporins (AQPs) are a family of small integral membrane proteins that primarily transport water across the cell membrane along osmotic gradients. Until now, 13 AQPs have been found in mammals (AQP0-12), some of which permit transcellular passage of glycerol and urea as well as water (AQP3, 7, 9, and 10) (6, 7). AQPs have been demonstrated to play a pivotal role in physiology and pathophysiology of body water balance (8). Experiments using AQP4-null mice revealed that AQP4 deletion protects from cellular (cytotoxic) brain edema produced by brain ischemia, but rather aggravates vasogenic (fluid leak) brain edema produced by brain tumor, providing strong evidence for AQP4 involvement in cerebral water balance (9). Based on the findings in brain edema, the implication of AQPs in myocardial water balance might also be postulated, but has not been determined.

In addition, the expression of AQP subtypes and their precise localization in myocardial tissue still remain unclear. In the mouse heart, the presence of AQP1, 4, 6, 7, 8, and 11 mRNA has so far been described, whereas only the presence of AQP1 and AQP4 was confirmed at the protein level (10, 11). However, for other AQPs, different results have been reported depending on the species and techniques used (12-14).

In this study, we characterized the expression patterns of AQP subtypes in normal mouse heart and investigated whether their expression levels change during the development and reabsorption of myocardial edema after MI.

MATERIALS AND METHODS

Animal preparation

All the procedures were approved by Dong-A University Medical School Institutional Animal Care and Use Committee (DIACUC-10-6-1). Total of 18 CD1 mice, 10-12 weeks of age, were used and divided into three groups; sham surgery group (Control, n = 6), 1-week MI group (MI-1W, n = 6) and 4-week MI group (MI-4W, n = 6). All the animals were anesthetized by intraperitoneal (IP) injection of 3.5% chloral hydrate (10 μL/g), endotracheally intubated, and mechanically ventilated using the Inspira-

pISSN 1011-8934
eISSN 1598-6357

Advanced Safety Ventilator (ASV, NP55-7050, Harvard Apparatus, Holliston, MA, USA), which supplied 0.25-0.30 mL room air 130 times per minute. The animal was moved onto its right side, and then the heart was exposed via a left thoracotomy. After removing the pericardium, the left anterior descending artery was visualized using a stereomicroscope (Nissho Optical, Kodama-gun, Japan), and occluded with a 9.0 nylon suture (Tyco Healthcare, North Haven, CT, USA). The suture was placed 0.3 mm distal to the atrioventricular junction. Occlusion was confirmed by observing the left ventricular pallor immediately after ligation. The chest was closed, the lungs reinflated, and the animal was moved into the prone position until spontaneous breathing occurred.

Measurement of cardiac function

Echocardiography analysis was performed baseline and each endpoint time using an echocardiography system with a Sonos 4500 and a 15-16 MHz transducer (Philips Corporation, Eindhoven, The Netherlands). The animals were sedated with anesthetic (3.5% chloral hydrate 1 mL/100 g, IP) and placed in the left lateral decubitus position. Parasternal long and short axis views were obtained in both M-mode and 2-dimensional echo images. Left ventricle end diastolic diameter (LVEDD) and left ventricle end systolic diameter (LVESD) were measured perpendicular to the long axis of the ventricle at the mid-chest level. Left ventricular ejection fraction (LVEF) was calculated automatically by the echocardiography system.

Tissue preparation

Animals were anesthetized and the thoracic cavity was opened to expose the heart. A 20-gauge needle connected with a micropump via a tube was inserted into the left ventricle, and the animal was slowly perfused with approximately 40-50 mL of phosphate buffered saline (PBS) until the fluid became clear. The hearts were cut into two equal transverse blocks from apex to base, either frozen in liquid nitrogen or fixed in 10% neutral buffered formalin and embedded in paraffin. Serial sections of 5-μm thickness were cut and used for further studies.

Assessment of myocardial water content

The hearts were removed at the different time points after MI and cut into two pieces just below the ligation suture. The lower half sections including the infarcted areas were weighed before (wet weight) and after drying to a constant weight in a desiccating oven at 65°C (dry weight). The percent myocardial water content was calculated as: (wet weight–dry weight) × 100/wet weight.

Immunostaining

Frozen sections were air-dried, fixed in ice-cold acetone and blocked with 5% bovine serum albumin before immunostaining. Paraffin sections were deparaffinized with xylene, and serially rehydrated in 100%, 95%, and 70% ethanol. For epitope retrieval, slides were immersed into coplin jar containing citrate buffer (10 mM sodium citrate, 0.05% Tween 20, pH 6.0) and boiled for 15 min. The jar was allowed to cool for 1 hr at room temperature (RT) and then slides were rinsed with washing buffer containing 0.025% Tween 20. After blocking for 2 hr, the sections were incubated with primary antibodies; rabbit polyclonal anti-AQP1 (1:300, Chemicon, Temecula, CA, USA), anti-AQP4 (1:300, Millipore, Billerica, MA, USA), anti-AQP6 (1:300, Chemicon), anti-AQP7 (1:300, Alpha Diagnostic, San Antonio, TX, USA) and anti-AQP9 (1:300, Alpha Diagnostic) overnight at 4°C. Secondary anti-rabbit horseradish peroxidase (HRP) linked IgG (1:100, Dako EnVision system, Glostrup, Denmark) was incubated for 1 hr at RT. The reaction was visualized with Dako DAB$^+$ chromogen (1:100). Tissue sections were mounted, and then visualized using digital scanning microscope (Scanscope, Aperio, Vista, CA, USA).

Western blot analysis

Frozen tissue was homogenized in ice-cold homogenization buffer (300 mM sucrose, 20 mM Hepes [pH 7.4]) containing protease inhibitor cocktail (Roche, Basel, Switzerland) using a dounce homogenizer in ice. Nuclei and debris were removed after low speed centrifugation (1,000 g for 10 min) at 4°C and the postnuclear supernatant was incubated with 2% Tween 20 for 1 hr in ice. The resultant crude membrane extract was loaded in each lane (50 μg per lane) to be separated by SDS-polyacrylamide gel electrophoresis (PAGE). After transferring the proteins onto a nitrocellulose membrane, the membrane was blocked with Tris-buffered saline-Tween (TBST; 20 mM Tris [pH 7.5], 145 mM NaCl, 0.05% Tween 20) containing 5% skim milk for 2 hr at RT, and then incubated with rabbit polyclonal anti-AQP1 (1:5,000), anti-AQP4 (1:5,000), anti-AQP6 (1:5,000) and anti-β-actin (1:2,500, Sigma-Aldrich, St. Louis, MO, USA), overnight at 4°C. After washing with TBST, the membranes were incubated with HRP-conjugated secondary antibodies (1:5,000, Cell Signaling, Danvers, MA, USA) for 45 min at RT and developed using a chemiluminescence detection system (Amersham Pharmacia Biotech, Little Chalfont, Bucks, UK).

Statistical analysis

All the data were expressed as mean ± standard error. The statistical significance of differences between groups was analyzed by the Student's t-test. Statistical significance was assumed at a value of $P < 0.05$.

RESULTS

AQP expression in normal heart

Immunostaining using antibodies against different AQP sub-

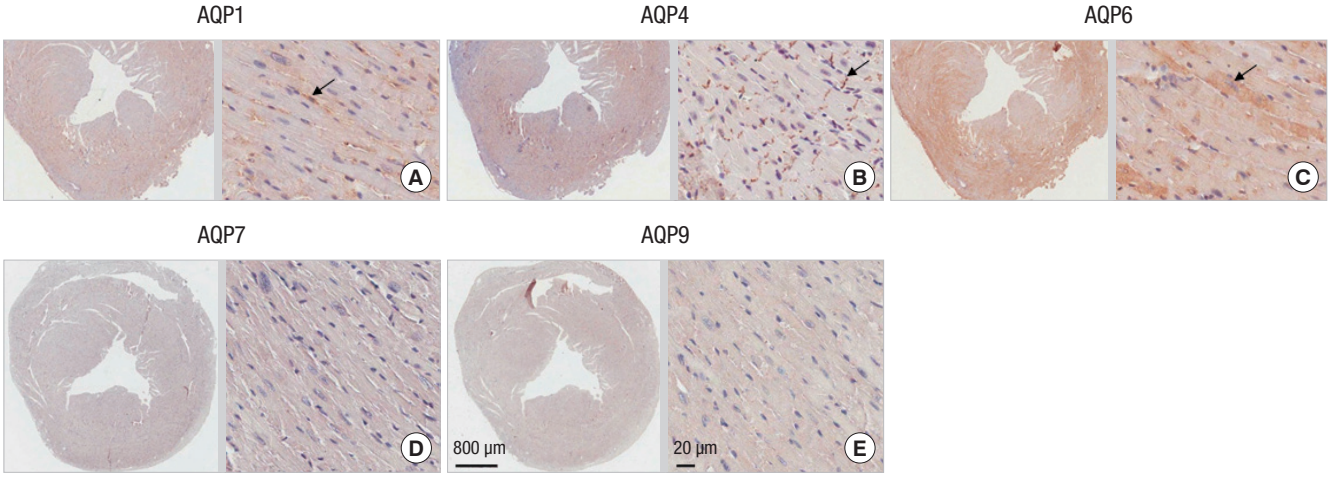

Fig. 1. Immunohistochemical analysis of aquaporins (AQPs) in normal mouse heart. Paraffin-embedded heart sections from normal mice were stained with antibodies against AQPs. AQP1 labels blood vessels and cytoplasm of cardiac myocytes (the arrow in **A**). AQP4 labeling is restricted to the intercalated discs (the arrow in **B**) and that of AQP6 distributes in striated pattern within the cardiac myocytes (the arrow in **C**). Neither AQP7 nor AQP9 are detected in the mouse heart (**D** and **E**).

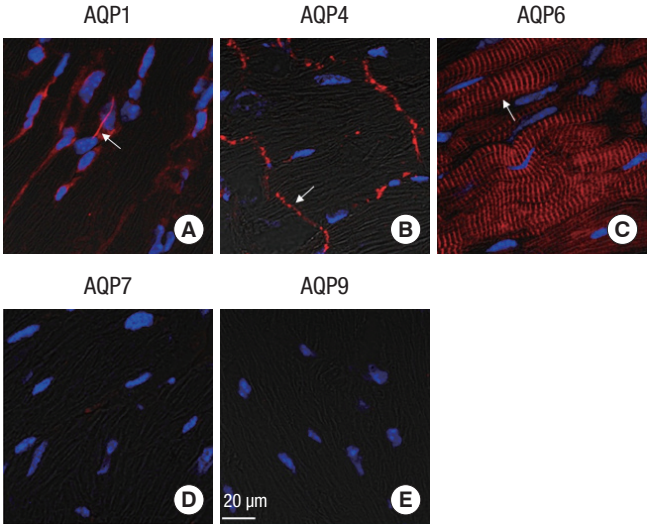

Fig. 2. Immunofluorescence analysis of aquaporins (AQPs) in normal mouse heart. Frozen heart sections from normal mice were stained with antibodies against AQPs. AQP1 labels blood vessels and cytoplasm of cardiac myocytes (the arrow in **A**). AQP4 labeling is restricted to the intercalated discs (the arrow in **B**) and that of AQP6 distributes in striated pattern within the cardiac myocytes (the arrow in **C**). Neither AQP7 nor AQP9 are detected in the mouse heart (**D** and **E**).

types was conducted to determine which AQPs are expressed in normal heart. As shown in Fig. 1 and 2, AQP1, AQP4 and AQP6 proteins were abundantly expressed in normal cardiac tissue. However, neither AQP7 nor AQP9 were expressed in normal CD1 mouse heart (Fig. 1D, E, and 2D, E). AQP1 expressed in vascular endothelial cells lining blood vessels and red blood cells within them (Fig. 1A, 2A). Weak AQP1 staining was also observed in the cytoplasm of cardiac myocytes. Anti-AQP4 antibody revealed prominent labeling at the intercalated discs between cardiac myocytes, exclusively on the side of transverse region (Fig. 1B, 2B). No significant density of anti-AQP4 stain was detected within the cytoplasm of cardiac myocytes in normal heart. AQP6 expressed abundantly and distributed throughout the cytoplasm of cardiac myocytes in a striated pattern (Fig. 1C, 2C).

Functional and histological changes after myocardial infarction

Hematoxylin-eosin stain shows that the pale area of infarction was well-demarcated from the surrounding normal-appearing red area, and replaced with early granulation tissue after 1 week (Fig. 3A, MI-1W). Widened inter-fiber space was prominent at 1 week after MI presumably due to the interstitial fluid accumulation. Necrotic cardiac myocytes with disappeared nuclei and less prominent striation were observed in infarct area, whereas infiltration of polymorphonuclear leukocytes and proliferation of fibroblasts were found at the periphery of the infarcted region. Four weeks following MI, necrotic tissue was totally absorbed and replaced with fibrous scar tissue so that myofibroblasts became the major cell type in infracted myocardium (Fig. 3A, MI-4W). Cardiac dilatation with expanded ventricular lumen was noticeable after 1 week and became more prominent after 4 week with the progressive thinning of the left ventricular wall.

We analyzed time-dependent changes of cardiac size and function after MI using echocardiography. LVESD and LVEDD, which are the parameters of left ventricular diameter, were increased in MI-induced groups, either MI-1W or MI-4W, when compared with those in sham-operated control group (Fig. 3B). Both values increased time-dependently up to 4 weeks after MI. LVEF, the most commonly used measure of overall cardiac function, was maximally reduced at 1 week post-MI (46.1% ± 4.9% in MI-1W; 73.1% ± 5.1% in control, $P < 0.01$), then slightly recovered at 4 weeks post-MI (52.7% ± 6.0% in MI-4W, $P < 0.05$).

For the assessment of myocardial edema, percent myocardial water content was measured after MI. Myocardial water con-

http://dx.doi.org/10.3346/jkms.2013.28.3.402

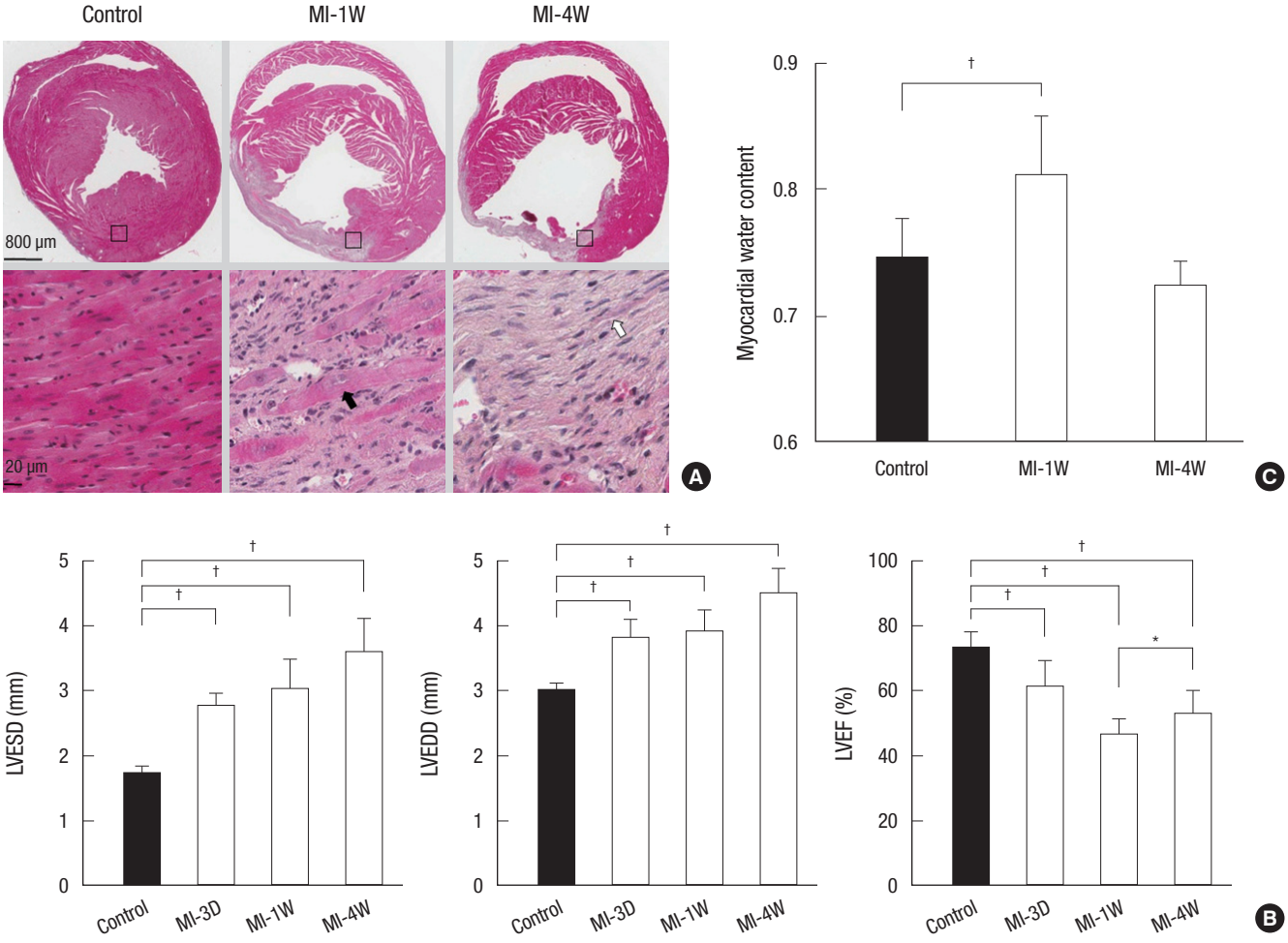

Fig. 3. Histopathological and functional changes following myocardial infarction (MI). (**A**) Hematoxylin-eosin stains of the heart sections from mice either sham-operated (control) or at 1 week (MI-1W) or 4 weeks (MI-4W) after MI induction. The area of acute infarction containing necrotic myocytes (the filled arrow) and neutrophil infiltrate at 1 week is replaced with proliferating myofibroblasts (the empty arrow) and fibrous tissue at 4 weeks. (**B**) Echocardiographic analysis of cardiac function. Both left ventricle end-systolic diameter (LVESD) and left ventricle end-diastolic diameter (LVEDD) increase steadily after MI, but left ventricular ejection fraction (LVEF) is maximally reduced at 1 week, then recovered after 4 weeks. Data represent mean ± SD from 6 mice per group. $^{*}P < 0.05$, $^{\dagger}P < 0.01$, compared with the corresponding value for control. (**C**) Myocardial water content (MWC) measured by wet-to-dry ratios. Data represent mean ± SD from 3 mice per group. $^{*}P < 0.05$, compared with the corresponding value for control.

tent increased by 8.7% at 1 week after MI and became slightly reduced at 4 weeks when compared with the control (Fig. 3C).

Changes of AQP expression after myocardial infarction

We next evaluated the MI-induced changes in expression patterns of AQP1, AQP4 and AQP6, which were confirmed to express in normal myocardium as shown in Fig. 1 and 2. The expression levels of all these AQPs increased following MI, not only at the periphery of infracted area but also in normal-appearing myocardium (Fig. 4). Although a slight up-regulation in cardiac myocytes was observed, MI-induced increase in AQP1 expression was mainly caused by increased signal from small blood vessels coursing between muscle fibers in non-infarcted areas up to 1 week (Fig. 4B). After 4 weeks of MI, much stronger staining intensity of AQP1 was observed inside cardiac myocytes (Fig. 4C). Intensity of AQP4 staining was also increased after MI so that intercalated discs looked more prominent (Fig. 4E). However, AQP4 staining pattern at intercalated discs appeared more undulated and widened at 1 week post-MI, presumably due to the interstitial edema. Interestingly, widely dispersed AQP4 staining became concentrated again at intercalated discs after 4 weeks (Fig. 4F). MI induced a dramatic up-regulation in AQP6 expression up to 4 weeks (Fig. 4H, I). Increased expression of AQP6 in cytoplasm made the sarcomeric striations of cardiac myocytes clearly discernible after MI. Individual sarcomeres as well as the space between them became widened after MI compared with those in sham operated control.

The MI-induced up-regulation of AQP expression was confirmed by western blot analysis. As shown in Fig. 5, regardless of the subtypes, AQPs showed increased expression after MI. However, the time courses of AQP expression following MI were different depending on the subtypes. Both AQP1 and AQP6 showed a stepwise increase in their expressions up to 4 weeks, whereas AQP4 reached peak expression at 1 week followed by a

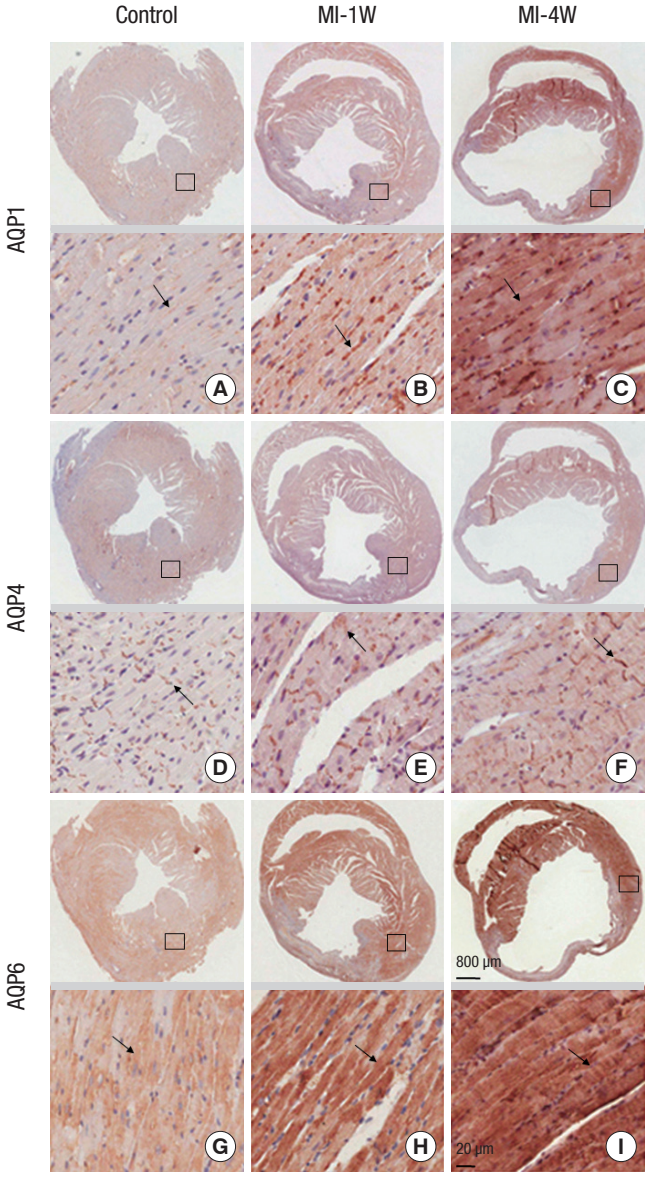

Fig. 4. Changes in AQP expression after myocardial infarction (MI). Immunohistochemical staining of AQP1, AQP4 and AQP6 on paraffin-embedded heart sections from mice either sham-operated (control, **A**, **D**, and **G**) or at 1 week (MI-1W, **B**, **E**, and **H**) or 4 weeks (MI-4W, **C**, **F**, and **I**) after MI induction. Labeling intensity of AQP1 in blood vessels and cardiac myocytes (arrows in **B** and **C**) increases with progression of MI. AQP4 labeling at intercalated discs is dispersed and undulated at 1 week (the arrows in **E**), but becomes more organized at 4 weeks (the arrow in **F**). AQP6 intensity in cardiac myocytes increases with the progression of MI, making the sarcomeric striations clearly discernible (arrows in **H** and **I**).

subsequent decline at 4 weeks.

DISCUSSION

The purpose of this study was to define the expression pattern of AQPs in normal heart and to investigate the changes in myocardial AQP expression after MI. We demonstrated here that AQP1, AQP4 and AQP6 are the main AQPs expressing in mouse heart and that the expressional level of these AQPs increases after MI with different time-dependent pattern, suggesting possible different roles for these AQPs on the pathogenesis of myocardial fluid accumulation accompanied by MI or on the post-infarction healing and remodeling process by facilitating myocardial fluid resorption.

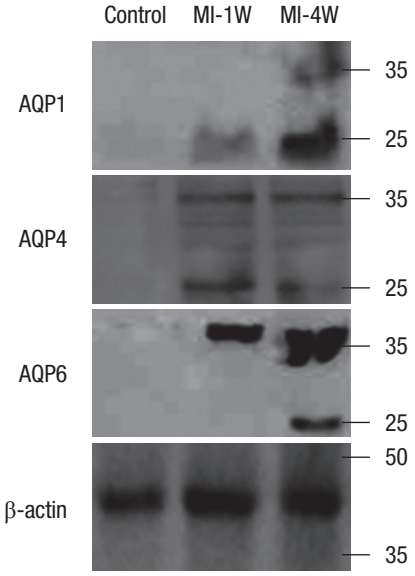

Fig. 5. Immunoblot analysis of AQP expression after myocardial infarction (MI). Immunoblotting of crude microsomal extract from myocardium of mice either sham-operated (control) or at 1 week (MI-1W) or 4 weeks (MI-4W) after MI induction. Expression levels of AQP1 and AQP6 increase steadily up to 4 weeks, but that of AQP4 peaks at 1 week then declines.

The subtype-specific expression of AQPs and their precise localization in heart have not been fully determined. Although the multiple AQP transcripts have been identified in human and mouse heart by RT-PCR analysis or Northern blot, only the presence of AQP1 was demonstrated at the protein level in human heart and that of AQP1, AQP4, and AQP7 in mouse heart (10, 13, 15). Moreover, their precise localization in myocardial tissue using immunohistochemistry has not been reported or remains equivocal except AQP1 (11). Here, we confirmed not only the presence of AQP1, AQP4, and AQP6 but also their detailed localization in mouse myocardium using immunohistochemistry and western blot. In accordance to the findings of others, we also observed the expression of AQP1 at the sarcolemma of cardiac myocytes, although its level is weaker than that in endothelia lining the vasculature in heart (10, 15). However, as for AQP4 localization, we obtained different results than the previous researchers in that AQP4 is highly enriched at the intercalated discs, not the entire sarcolemma of cardiac myocytes as previously reported (10, 15). Whereas AQP4 localizes to the perivascular endfeet of astrocytes and skeletal muscle sarcolemma by binding syntrophin associated with the dystrophin-glycoprotein complex (17, 18), in cardiac tissue, AQP4 distributes exclusively at the intercalated discs. Recently, it has been reported that the main cardiac voltage-gated sodium channel,

http://dx.doi.org/10.3346/jkms.2013.28.3.402

$Na_v1.5$, is anchored to either the lateral membranes by binding syntrophin-dystrophin complex or the intercalated disc by binding synapse-associated protein 97 (SAP97) through PSD-95/Discs-large/ZO-1 (PDZ) domain binding motif in cardiac myocytes (19). Since AQP4 also has PDZ domain binding sequence at the C-terminal (20), binding of AQP4 to SAP97 might be one possibility for its localization to the intercalated disc.

Although the presence of AQP6 transcript was suggested previously by RT-PCR (10), we first observed that AQP6 proteins express in heart and localize inside the cardiac myocytes. AQP6 was originally identified as a homolog of AQP2 and expresses mainly in the intracellular vesicles of acid-secreting type A-intercalated cells of renal collecting ducts, colocalizing with H^+-ATPase (21). AQP6 is permeable to anionic ions, especially nitrate, as well as water (22). AQP6 has been reported to express in synaptic vesicles and participate in their swelling with AQP1 (23). The possible roles of AQP6 in intracellular pH regulation, nitrate efflux or vesicular transport in cardiac myocytes remain to be established.

It is difficult to detect the myocardial edema-induced changes of ventricular wall thickness in mouse heart with echocardiography, since even clinically significant myocardial edema results in a 10% increase in ventricular wall thickness, which corresponds to 1 mm in adult human heart (24). We measured the myocardial water content using wet-to-dry weight ratio in mice and observed that myocardial water content increased by 8.7% at 1 week after MI. We also evaluated the post-infarction cardiac dysfunction with echocardiography and found that left ventricular function is maximally reduced at 1 week post MI and slightly recovers 4 weeks later. Our finding coincides well with the time course of the postinfarction myocardial edema reported by Nilsson et al. (25), who measured the myocardial edema using the magnetic resonance imaging in human. They found that myocardial edema was greatest 1 week after the infraction with gradual decline during the following months, but lasted surprisingly long with a median duration of 6 months. Based on the report demonstrating that 3.5% increase in myocardial water content resulted in 40% decrease of cardiac output (26), we can assume that the degree of myocardial edema developed in our study is more severe.

Despite the presence of several AQPs in myocardium, their roles in development and resolution in myocardial ischemia have not been established yet. We demonstrated here the up-regulation of cardiac AQPs following MI. However, time-dependent patterns in their expression were different. The time course of AQP4 expression correlated well to that of left ventricular dysfunction which is maximal at 1 week followed by a partial recovery at 4 weeks, whereas AQP1 and AQP6 increased steadily with time after MI irrespective of cardiac function. Warth et al. (27) also observed upregulation of AQP4 mRNA and protein after 2 hr of ischemia and 3 hr of reperfusion, but showed anti-AQP4 immunoreactivity decorating the whole sarcolemma of ischemic myocytes. In addition to the expression level, we found MI-induced changes in the distribution pattern of AQP4 proteins. The pattern of anti-AQP4 staining at the intercalated discs has changed to give more undulating appearance following MI, presumably due to integrity loss of the intercalated discs. The dissipation of gap junction and remodeling of intercalated discs was frequently observed following MI (28). As AQP4 is a well-known player for development of cellular edema following cerebral ischemia (29), polarized localization of AQP4 is worthy of note for myocardial water and ionic homeostasis. It was suggested that AQP4 in astrocyte endfeet not only closely associates but also functionally interacts with the inward rectifying potassium channel, Kir4.1, for extracellular K^+ buffering (30). In cardiac tissue, AQP4 might also work in concert with adjacent ion channels and gap junctions, and help to maintain the constant volume and ionic concentration of interstitial fluid at intercalated discs by facilitating water transport across the membrane for normal excitation and conduction or for the tolerance against ischemic insults.

MI-induced increase of AQP1 expression was not as strong as the other two AQPs, and mainly confined to the blood vessel, which was supportive of the previous findings (31). The abundance of AQP1 protein in cardiac tissue after MI reflects the increased numbers of microvasculature in response to hypoxia and might contribute to the interstitial fluid accumulation. Implication of AQP1 for the development of lung edema has been described (32). MI-induced increase of AQP6 expression was the most prominent among the AQPs tested, and gave a clear and distinct striation pattern to cardiac myocytes with the widening of sarcomeres and the space between them, presumably due to cell swelling. After MI, accumulation of acid metabolites such as lactate due to the death of ischemic myocytes would induce acidification of cytoplasm pH, which might trigger AQP6 to permeate anions including nitrate, a metabolite from nitric oxide. However, the role of AQP6 in cardiac ischemia and post-infarct edema formation, either as a water channel or an anion channel, needs to be elucidated.

The possibility cannot be excluded that the observed up-regulation of AQP1, AQP4, and AQP6 at the early stages of ischemia might act as a protective mechanism of heart from developing post-infarct edema via facilitating water shift for its drainage towards lymphatics. However, it might more reasonable to explain AQP up-regulation as a contributing factor to developing post-infarct edema as the inwardly directed osmotic gradients for water flow would be created due to the rapid accumulation of acid metabolites after MI (33). To get more insight into the role of AQPs in myocardial edema formation, further experiments will be necessary to evaluate the levels of cardiac AQPs in the diverse pathologies of the heart associated with exceeding water accumulation in the myocardium using subtype-specific

AQP null mice. Manipulating the expression levels of AQPs to avoid cell swelling might be a possible strategy for the cardiac protection and ischemic preconditioning.

ACKNOWLEDGMENTS

The authors have no conflicts of interest to disclose.

REFERENCES

1. Mehlhorn U, Geissler HJ, Laine GA, Allen SJ. *Myocardial fluid balance. Eur J Cardiothorac Surg 2001; 20: 1220-30.*
2. Garcia-Dorado D, Andres-Villarreal M, Ruiz-Meana M, Inserte J, Barba I. *Myocardial edema: a translational view. J Mol Cell Cardiol 2012; 52: 931-9.*
3. Bijnens B, Sutherland GR. *Myocardial oedema: a forgotten entity essential to the understanding of regional function after ischaemia or reperfusion injury. Heart 2008; 94: 1117-9.*
4. Møller JE, Egstrup K, Køber L, Poulsen SH, Nyvad O, Torp-Pedersen C. *Prognostic importance of systolic and diastolic function after acute myocardial infarction. Am Heart J 2003; 145: 147-53.*
5. St John Sutton M. *Quest for diastolic prognostic indicators of clinical outcome after acute myocardial infarction. Circulation 2008; 117: 2570-2.*
6. Hara-Chikuma M, Verkman AS. *Physiological roles of glycerol-transporting aquaporins: the aquaglyceroporins. Cell Mol Life Sci 2006; 63: 1386-92.*
7. Ishibashi K, Hara S, Kondo S. *Aquaporin water channels in mammals. Clin Exp Nephrol 2009; 13: 107-17.*
8. Verkman AS. *Novel roles of aquaporins revealed by phenotype analysis of knockout mice. Rev Physiol Biochem Pharmacol 2005; 155: 31-55.*
9. Manley GT, Fujimura M, Ma T, Noshita N, Filiz F, Bollen AW, Chan P, Verkman AS. *Aquaporin-4 deletion in mice reduces brain edema after acute water intoxication and ischemic stroke. Nat Med 2000; 6: 159-63.*
10. Butler TL, Au CG, Yang B, Egan JR, Tan YM, Hardeman EC, North KN, Verkman AS, Winlaw DS. *Cardiac aquaporin expression in humans, rats, and mice. Am J Physiol Heart Circ Physiol 2006; 291: H705-13.*
11. Egan JR, Butler TL, Au CG, Tan YM, North KN, Winlaw DS. *Myocardial water handling and the role of aquaporins. Biochim Biophys Acta 2006; 1758: 1043-52.*
12. Ma T, Yang B, Verkman AS. *Cloning of a novel water and urea-permeable aquaporin from mouse expressed strongly in colon, placenta, liver, and heart. Biochem Biophys Res Commun 1997; 240: 324-8.*
13. Nejsum LN, Elkjaer M, Hager H, Frokiaer J, Kwon TH, Nielsen S. *Localization of aquaporin-7 in rat and mouse kidney using RT-PCR, immunoblotting, and immunocytochemistry. Biochem Biophys Res Commun 2000; 277: 164-70.*
14. Liu K, Nagase H, Huang CG, Calamita G, Agre P. *Purification and functional characterization of aquaporin-8. Biol Cell 2006; 98: 153-61.*
15. Au CG, Cooper ST, Lo HP, Compton AG, Yang N, Wintour EM, North KN, Winlaw DS. *Expression of aquaporin 1 in human cardiac and skeletal muscle. J Mol Cell Cardiol 2004; 36: 655-62.*
16. Sheikh F, Ross RS, Chen J. *Cell-cell connection to cardiac disease. Trends Cardiovasc Med 2009; 19: 182-90.*
17. Neely JD, Amiry-Moghaddam M, Ottersen OP, Froehner SC, Agre P, Adams ME. *Syntrophin-dependent expression and localization of Aquaporin-4 water channel protein. Proc Natl Acad Sci U S A 2001; 98: 14108-13.*
18. Adams ME, Mueller HA, Froehner SC. *In vivo requirement of the alpha-syntrophin PDZ domain for the sarcolemmal localization of nNOS and aquaporin-4. J Cell Biol 2001; 155: 113-22.*
19. Petitprez S, Zmoos AF, Ogrodnik J, Balse E, Raad N, El-Haou S, Albesa M, Bittihn P, Luther S, Lehnart SE, et al. *SAP97 and dystrophin macromolecular complexes determine two pools of cardiac sodium channels Nav1.5 in cardiomyocytes. Circ Res 2011; 108: 294-304.*
20. Shi LB, Skach WR, Ma T, Verkman AS. *Distinct biogenesis mechanisms for the water channels MIWC and CHIP28 at the endoplasmic reticulum. Biochemistry 1995; 34: 8250-6.*
21. Ohshiro K, Yaoita E, Yoshida Y, Fujinaka H, Matsuki A, Kamiie J, Kovalenko P, Yamamoto T. *Expression and immunolocalization of AQP6 in intercalated cells of the rat kidney collecting duct. Arch Histol Cytol 2001; 64: 329-38.*
22. Ikeda M, Beitz E, Kozono D, Guggino WB, Agre P, Yasui M. *Characterization of aquaporin-6 as a nitrate channel in mammalian cells. Requirement of pore-lining residue threonine 63. J Biol Chem 2002; 277: 39873-9.*
23. Jeremic A, Cho WJ, Jena BP. *Involvement of water channels in synaptic vesicle swelling. Exp Biol Med (Maywood) 2005; 230: 674-80.*
24. Pelliccia A, Maron BJ, Spataro A, Proschan MA, Spirito P. *The upper limit of physiologic cardiac hypertrophy in highly trained elite athletes. N Engl J Med 1991; 324: 295–301.*
25. Nilsson JC, Nielsen G, Groenning BA, Fritz-Hansen T, Sondergaard L, Jensen GB, Larsson HB. *Sustained postinfarction myocardial oedema in humans visualised by magnetic resonance imaging. Heart 2001; 85: 639-42.*
26. Laine GA, Allen SJ. *Left ventricular myocardial edema: lymph flow, interstitial fibrosis, and cardiac function. Circ Res 1991; 68: 1713-21.*
27. Warth A, Eckle T, Köhler D, Faigle M, Zug S, Klingel K, Eltzschig HK, Wolburg H. *Upregulation of the water channel aquaporin-4 as a potential cause of postischemic cell swelling in a murine model of myocardial infarction. Cardiology 2007; 107: 402-10.*
28. Matsushita T, Oyamada M, Fujimoto K, Yasuda Y, Masuda S, Wada Y, Oka T, Takamatsu T. *Remodeling of cell-cell and cell-extracellular matrix interactions at the border zone of rat myocardial infarcts. Circ Res 1999; 85: 1046-55.*
29. Papadopoulos MC, Verkman AS. *Aquaporin-4 and brain edema. Pediatr Nephrol 2007; 22: 778-84.*
30. Strohschein S, Hüttmann K, Gabriel S, Binder DK, Heinemann U, Steinhäuser C. *Impact of aquaporin-4 channels on K+ buffering and gap junction coupling in the hippocampus. Glia 2011; 59: 973-80.*
31. Ran X, Wang H, Chen Y, Zeng Z, Zhou Q, Zheng R, Sun J, Wang B, Lv X, Liang Y, et al. *Aquaporin-1 expression and angiogenesis in rabbit chronic myocardial ischemia is decreased by acetazolamide. Heart Vessels 2010; 25: 237-47.*
32. Borok Z, Verkman AS. *Lung edema clearance: 20 years of progress: invited review: role of aquaporin water channels in fluid transport in lung and airways. J Appl Physiol 2002; 93: 2199-206.*
33. Suleymanian MA, Baumgarten CM. *Osmotic gradient-induced water permeation across the sarcolemma of rabbit ventricular myocytes. J Gen Physiol 1996; 107: 503-14.*

 http://dx.doi.org/10.3346/jkms.2013.28.3.402